

Direct Observation of Subluminal and Superluminal Velocity Swinging in Coupled Mode Optical Propagation

Andrea Melloni*

Dipartimento di Elettronica e Informazione, Politecnico di Milano, Via Ponzio 34/5, 20133 Milano, Italy

Francesco Morichetti

*Dipartimento di Elettronica e Informazione, Politecnico di Milano, Via Ponzio 34/5, 20133 Milano, Italy
and CoreCom, Via G. Colombo, 81, Milano 20133, Italy*

(Received 12 December 2006; revised manuscript received 2 March 2007; published 26 April 2007)

A direct measure of the periodical power exchange between optical coupled modes with different polarization states is presented. The effects of the coupling on the relative velocity of the two modes are experimentally observed and analytically explained. Coupled modes are discovered to periodically attract and repel under the effect of swinging subluminal and superluminal regimes. The measurement technique is based on a novel polarization-sensitive scheme for optical low-coherence interferometry, providing in time domain the complex amplitudes of the interacting fields.

DOI: [10.1103/PhysRevLett.98.173902](https://doi.org/10.1103/PhysRevLett.98.173902)

PACS numbers: 42.25.Bs, 07.60.Ly, 42.25.Kb, 42.81.Gs

The well-established belief that superluminal effects can arise only in passive systems with absorption or reflection or in active transparent media has been recently dismantled, by proving that the energy transfer between (coupled) modes provides a sufficient condition for anomalous dispersion [1]. In this pioneering experiment, the superluminal group delay of a wave in a photonic crystal was inferred from spectral domain measurements, carried out at microwave frequencies, and no causality violation was demonstrated by a vectorial formulation of the Kramers-Kronig relations. However, the instantaneous group velocity in coupled wave systems has never been measured so far. As shown in this Letter, this lack of information hinders the full comprehension of the mechanisms underlying coupling-induced superluminality, and the ultimate limit to light speed in such systems is still an open issue.

Here we show, for the first time, that superluminal propagation in coupled wave systems can not last indefinitely. The instantaneous group velocity is not constant in time, but periodically swings from superluminal to subluminal regimes under the effect of the mutual power transfer. For clarity's sake, the term superluminal (subluminal) is here generally referred to propagation with group velocity higher (lower) than the speed of light in the optical medium, that in the reported experiment is an optical waveguide. Attraction and repulsion of the interacting fields is experimentally demonstrated by a direct time-resolved observation of coupled mode propagation at optical frequencies. The complex amplitude of guided modes with different polarization states, coupled by waveguide bending in a ring resonator [2], is measured by a novel time domain technique based on polarization-sensitive Optical Low-Coherence Interferometry (OLCI). Experimental results are interpreted by means of the Coupled Mode Theory (CMT) [3], and conditions for propagation at velocity well above the vacuum speed of light c are discussed.

The proposed technique provides a direct measurement of the polarization coupling matrix $\mathbf{H} = [h_{uv}]$ ($u, v = e, m$), which relates the complex amplitudes of the TE and TM polarized fields at the input and the output of an optical device [4]. The four terms h_{uv} are time resolved by exploiting the group velocity difference between the two axes of a polarization maintaining (PM) fiber, as sketched in Fig. 1(a). The probe signal is the autocorrelation function $\gamma(\tau)$ of an optical source with coherence time τ_c . Two PM fibers, namely PM1 and PM2, are employed to couple light into and out of the device under test (DUT), respectively. Let τ_i ($i = 1, 2$) be the relative delay between the two modes of the fiber PM_i . The optical axes of both fibers are aligned to the axes of the device, so as to maximize the overlap between the slow (fast) axis fiber mode and the TE (TM) mode of the device. The TE and TM modes are excited with a relative delay τ_1 . The cross coupling between the PM1 fast (slow) axis mode and the PM2 slow (fast) axis mode reveals the presence of polarization cou-

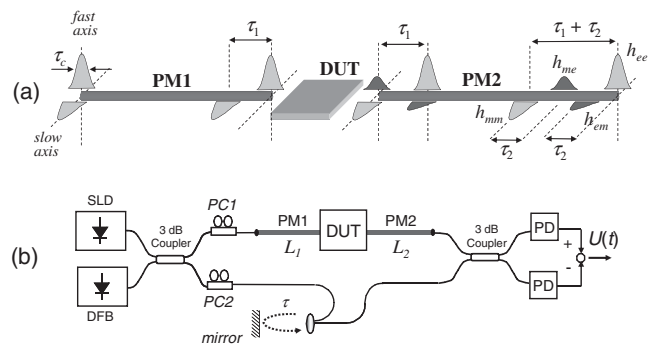


FIG. 1. Polarization-sensitive OLCI: schematic of the relative time delay introduced by the two PM fibers at the input and output of the DUT (a) and OLCI experimental setup for measurements of polarization coupling in optical devices (b).

pling in the DUT. These cross-polarization states, indicated in darker gray in Fig. 1(a), are separated from the input polarization states by a relative delay τ_2 . The amplitude and the phase of $h_{uv}(\tau)$ are measured by the OLCI setup shown in Fig. 1(b), which gives the cross correlation [5]

$$U(\tau) = \text{Re}[\gamma(\tau) * H(\tau)] \cos\left(\frac{2\pi c\tau}{\lambda_0}\right) \quad (1)$$

between a low-coherence reference field and the same field travelling in the DUT. In Eq. (1), $H(\tau) = h_{ee}(\tau) + h_{em}(\tau - \tau_2) + h_{me}(\tau - \tau_1) + h_{mm}[\tau - (\tau_2 + \tau_1)]$ is the DUT polarization dependent impulse response, λ_0 is the central wavelength of the optical source and the asterisk denotes time convolution. If $\tau_c < |\tau_1 - \tau_2|$, all the four terms h_{uv} are resolved in time and can be directly measured.

This technique was employed for the investigation of polarization coupling effects in bent waveguides. The origin of these phenomena lies in the different hybridness of the straight waveguide modes and the bend modes [6]. Along the bend, a spatially periodic power exchange between the quasi-TE and quasi-TM modes of the straight waveguide, hereinafter simply referred to as TE and TM, is analytically predicted by the CMT [3] and confirmed by electromagnetic simulations [7]. The beat length of the conversion process is $L_B = \pi/\delta = \pi/(\kappa_p^2 + \Delta\beta^2/4)^{1/2}$, where κ_p is the field polarization coupling coefficient and $\Delta\beta = \beta_{\text{TE}} - \beta_{\text{TM}}$ is the difference of the propagation constants. In our experiment, the bent waveguide of an integrated phase shifter was used. The device, shown in the inset of Fig. 2, consists of a ring resonator with radius ρ coupled with a bus waveguide by a field coupling coefficient $-jt$. The elements of the matrix \mathbf{H} , describing the

relations between the polarization state of the input fields and the fields outgoing the resonator after n ($n \geq 1$) round-trips, can be expressed as

$$h_{ee,n} = h_{mm,n}^* = -t^2 z^{-n} [\cos(n\phi) - jR \sin(n\phi)], \quad (2)$$

$$h_{em,n} = h_{me,n} = -t^2 z^{-n} [-jS \sin(n\phi)], \quad (3)$$

where $R = \Delta\beta/2\delta$ is related to the asynchrony of the coupling process, $S = \kappa_p/\delta$, $\phi = 2\pi\rho\delta$, and $z^{-1} = \exp[-j\pi\rho(\beta_{\text{TE}} + \beta_{\text{TM}})]$ is the ring round-trip delay [8].

The OLCI experimental setup is schematically shown in Fig. 1(b). It consists of a fiber Mach-Zehnder interferometer, where a DFB source is used in addition to the low coherent Super Luminescent Diode (SLD) to allow a sub-wavelength measure of the delay τ in the reference arm. The SLD has a coherence time $\tau_c = 113$ fs and central wavelength $\lambda_0 = 1538$ nm, the DFB has 5 MHz linewidth and is centered at 1310.25 nm. The angular accuracy ($\pm 2^\circ$ degrees) in positioning the axes of the PM fibers guarantees less than -30 dB polarization crosstalk at the DUT input. A first polarization controller (PC1) is inserted into the DUT arm to adjust the amplitude of the PM1 modes; the second polarization controller (PC2) is used to maximize the interference with the field in the reference arm, where only low-birefringence fibers are employed. Two photodetectors (PD) in differential configuration are used to double the amplitude of the interference pattern and to remove common mode noise.

In the next part of the Letter, experimental results on a ring-resonator phase shifter realized in silicon oxynitride (SiON) technology are reported. The free spectral range of the device, with bending radius $\rho = 274.5 \mu\text{m}$, is FSR = 100 GHz. The waveguide is rib-shaped, with 6% refractive index contrast and 25° slanted sidewalls. Both the strong index contrast and the asymmetry in the direction orthogonal to the bend plane increase the bend mode hybridness and favor the TE-TM coupling [4]. More details on technology and design of the waveguide can be found in Ref. [9]. The measured radiation loss is below 0.045 dB/rad for bending radii down to $\rho = 200 \mu\text{m}$, so that the lossless approximation for the CMT model is adopted in the discussion of the results.

Figure 2 shows the experimental OLCI trace of the ring resonator. The measure consists of an infinite sequence of interference patterns S_n , spaced by the 10 ps ring round-trip delay, the n -th set corresponding to the light outgoing the resonator after n round-trips. The four peaks within each set S_n are due to the time splitting given by the PM fibers, as sketched in Fig. 1(a), and provide a direct measure of the terms $h_{uv,n}$ of Eqs. (2) and (3). As n increases, the time (space) evolution of the TE and TM complex amplitudes along the bend is tracked. Polarization coupling effects are revealed by the change of the relative $h_{uv,n}$ amplitudes. Intensity is proportional to the squared envelope of the OLCI trace, whereas phase information can be

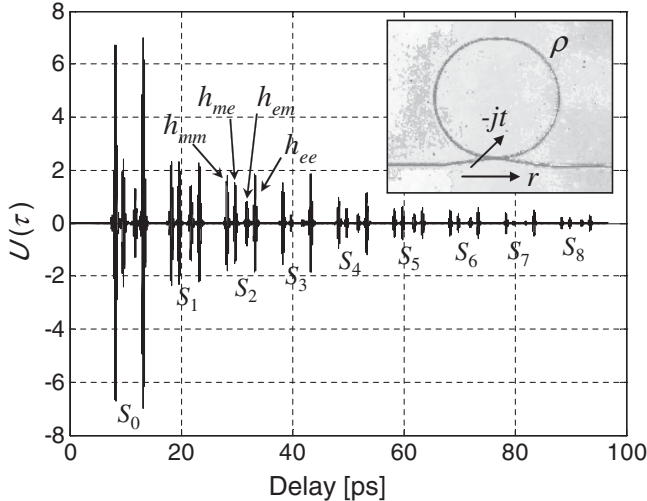


FIG. 2. OLCI interference pattern of the phase shifter (FSR = 100 GHz) shown in the inset. Each set S_n , corresponding to the field outgoing the resonator after n round-trips, contains the four time-resolved contributions $h_{uv,n}$ disclosed in Fig. 1(a).

extracted from the interference fringes underneath each peak. The output field can be observed only after an integer number n of round-trips, so that the resonator radius ρ fixes the sampling rate of the measurement. The resolution of the OLCI technique is ultimately given by the source coherence time τ_c , which limits the maximum ring FSR to $\tau_c^{-1}/2$ (nearly 4.5 THz in our experiment). The two peaks $h_{em,0}$ and $h_{me,0}$ in S_0 , corresponding to the light not coupled into the resonator, are due to a bend in the bus waveguide, which is responsible for some polarization coupling outside the resonator.

From the time trace of Fig. 2, a deep insight into the properties of coupled mode propagation can be inferred. The power exchange between the two polarization states is described by the conversion efficiency matrix \mathbf{K} , defined as $K_{uu} = |h_{uu}|^2 / (|h_{uu}|^2 + |h_{uv}|^2)$ (diagonal components) and $K_{uv} = |h_{uv}|^2 / (|h_{uu}|^2 + |h_{uv}|^2)$ (off-diagonal components), with $u, v = e, m$ [4]. Figure 3(a) shows the measured periodical conversion efficiency of an input TM mode toward the output TE (K_{me} , circles) and TM (K_{mm} , squares) modes. An analogous behavior is observed for K_{em} and K_{mm} , not shown in the figure for clarity's sake. The beat length $L_B = 6.78$ mm is about 3 times the ring's optical length. The values $\kappa_p = 388 \text{ m}^{-1}$ and $\Delta\beta = 608 \text{ m}^{-1}$ were retrieved by numerical fitting with the CMT model [4] (solid lines), showing that up to 62% of the input power is rotated to the orthogonal polarization state. Total power transfer is predicted in the synchronous coupling case $\Delta\beta(\lambda_0) = 0$, as shown in Fig. 3(a) by the dashed-dotted line. The effects of polarization rotation on the spectral response of the resonator have been recently reported [8].

In addition to this well-known power bouncing, we found also an inexperienced swinging of the group velocity. Figure 3(b) shows the measured relative delay $\tau_r = \tau_{\text{TM}} - \tau_{\text{TE}}$ (marks), directly evaluated as the time interval between the h_{mm} and h_{ee} envelopes of Fig. 2. In the CMT model (solid line) the parameters recovered from the fitting of Fig. 3(a) are used. In the absence of mode coupling ($\kappa_p = 0$), the delay of the slower mode, TM polarized in the experiment, is expected to increase linearly by 5 fs per roundtrip (dashed line) because of the group birefringence $B_g = 7.4 \times 10^{-4}$. Actually, measurements show that the two modes periodically approach each other with period L_B . This result is in agreement with the CMT model, stating that the delay between coupled modes with different group velocities depends on the power transfer. It can be derived from Eqs. (2) that, at the maxima of K_{me} , $\tau_{r,M}$ coincides with delay τ_0 in the absence of polarization coupling ($\kappa_p = 0$, dashed line). For small values of R , defined after Eq. (3), $\tau_{r,M}$ scales as $\tau_0 R^{-1}$. When K_{me} is minimum, the delay reduces to $\tau_{r,m} = R^2 \tau_0 = 0.38 \tau_0$. In the synchronous coupling case $\Delta\beta(\lambda_0) = 0$ (dashed-dotted line), indefinitely large delays, either positive or negative, are predicted. Nevertheless, because of the total

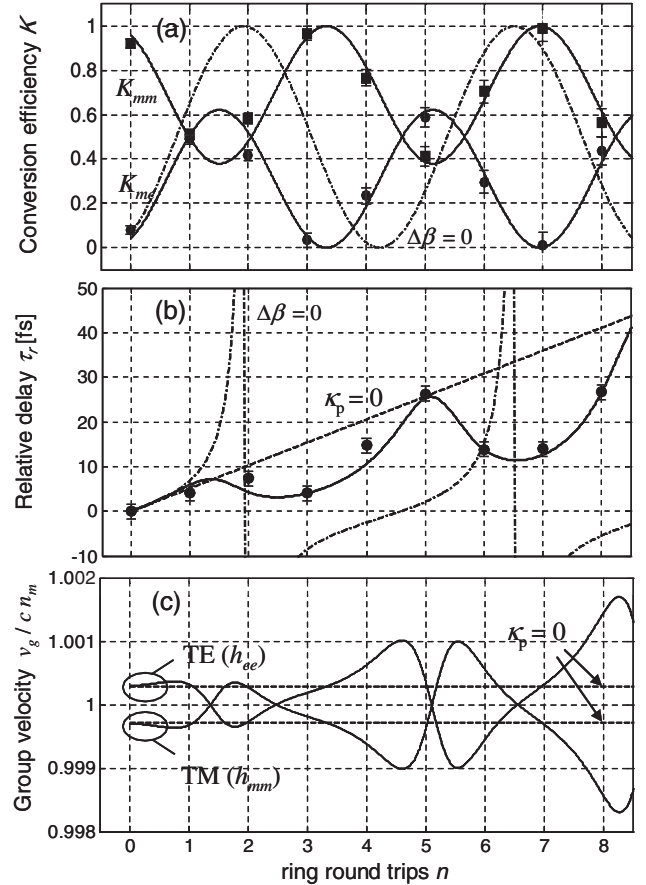


FIG. 3. Coupled mode propagation along the bend of the ring-resonator phase shifter of Fig. 2. (a) Measured conversion efficiency K_{me} (circles) and K_{mm} (squares). In solid lines, the CMT numerical fitting is reported. The dashed-dotted line shows the predicted conversion in the synchronous coupling case. (b) Measured relative group delay τ_r between the TM and TE coupled modes (circles) and CMT prediction (solid line). Dashed line and dashed-dotted line show the relative delay in the case $\kappa_p = 0$ and $\Delta\beta(\lambda_0) = 0$, respectively. (c) Normalized instantaneous group velocity of the coupled (solid lines) and uncoupled (dashed lines) modes in the bend.

power transfer, the relative delay comes back to the input value after an integer number of beat lengths ($n = 4, 6$).

A simple explanation of this behavior is given by Fig. 4, which discloses the envelope of the output TM ($h_{mm,n}$, solid lines) and TE ($h_{me,n}$, dashed lines) modes, calculated by the CMT model. The normalized fields at the input section of the bend are $h_{mm,0}$ and $h_{me,0}$. After $n = 5$ round trips, K_{me} is maximum (see Fig. 3(a)) and the peak power of the TE mode ($|h_{me,5}|^2$) is 62% of the input power. Because of the higher speed of the TE mode, the conversion process is more efficient nearby the leading edge of the TM envelope, where the TE mode grows up and the TM mode loses most of its power. The TM envelope is partially reshaped, its peak is pushed backward, and $\tau_{r,M} = 24$ fs after 5 round trips, in agreement with Fig. 3(b). When the

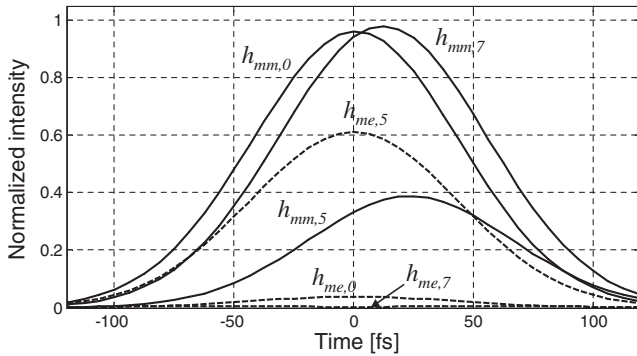


FIG. 4. CMT simulation of the temporal envelopes of the coupled modes $h_{mm,n}(\tau)$ and $h_{me,n}(\tau)$ after $n = 0, 5$ and 7 round trips in the ring resonator of Fig. 2.

power transfer reverses, the TM mode receives power mainly in the leading edge, and its envelope is forwardly distorted. After 7 round trips, $h_{me,7}$ is almost zero, all the power is back converted to TM ($|h_{mm,7}|^2 = 1$), and the delay drops to $\tau_{r,m} = 13$ fs.

Figure 3(c) shows the group velocity v_g calculated by the CMT and normalized to the average velocity $c/n_m = 2c/(n_{g,e} + n_{g,m})$, $n_{g,e} = 1.549$, and $n_{g,m} = n_{g,e} + B_g$ being the effective group index of the uncoupled TE and TM modes in the straight waveguide, respectively. Dashed lines show the group velocities of the TM (slower) and TE (faster) mode in the absence of polarization coupling. The cross-polarization states, h_{em} and h_{me} , are found to propagate at constant velocity c/n_m . On the contrary, the group velocity of the h_{ee} and h_{mm} fields, strongly depends on the power exchange. When K_{me} (K_{em}) is minimum, the h_{mm} (h_{ee}) velocity coincides with the velocity of the uncoupled mode $c/n_{g,m}$ ($c/n_{g,e}$) because all the power is back converted to the input mode. At local maxima or minima of τ_r , where the envelope distortion reverses, the velocities of all the fields h_{uv} coincides with c/n_m . Group velocities higher than those of the uncoupled modes can be reached and superluminal propagation is observed, as a consequence of the envelope reshaping [10]. The TM mode (h_{mm}) is superluminal when receiving power from the TE mode (h_{me}), while the TE mode (h_{ee}) is superluminal when providing power to the TM mode (h_{em}). The swing of the group velocity from subluminal to superluminal regime is responsible for the periodical attraction and repulsion in such systems is given by the synchronous coupling case. With reference to Fig. 3(b) (dashed-dotted line), the delay of the input TM mode progressively increases as long as TM power drops to zero, then back-converted TM power appears with a negative delay. From the point of view of the TM mode, this instantaneous spatial advancement occurs with an infinite group velocity. However, the TM (TE) average group velocity, evaluated along an integer number

of beat lengths, is always found to range between the uncoupled wave speed $c/n_{g,m}$ ($c/n_{g,e}$) and the synchronous coupling speed c/n_m , which are both below the vacuum light speed c .

In conclusion, by means of a direct time-resolved measure, the periodical swing of the instantaneous group velocity from subluminal to superluminal regime in coupled mode systems has been demonstrated. Negative delays and infinite instantaneous velocities are also predicted, but with an average velocity always below the vacuum light speed. To the author's knowledge, this result not only represents the first observation of superluminal propagation in systems at optical frequencies with neither absorption nor reflection, but also provides the first experimental validation of the CMT model for polarization coupling in optical bends. To overcome the limitation of the presented OLCI measurement, whose resolution is fixed by the bending radius of the optical resonator, advanced interferometrical techniques are required. For example, phase-sensitive near-field scanning optical microscopy, recently applied to measure the velocity of the optical modes of a photonic crystal waveguide, allows field inspection in each point of the waveguide, but at the cost of a significantly higher complexity in the experimental setup [11].

The authors are indebted to Prof. M. Martinelli for valuable discussions and continuous encouragement. This research has been partly supported by the European Contract SPLASH within the 6th FP.

*Electronic address: melloni@elet.polimi.it

- [1] D. R. Solli, C. F. McCormick, C. Ropers, J. J. Morehead, R. Y. Chiao, and J. M. Hickmann, Phys. Rev. Lett. **91**, 143906 (2003).
- [2] T. Yoneyama, H. Tamaki, and S. Nishida, IEEE Trans. Microwave Theory Tech. **34**, 876 (1986).
- [3] W. W. Lui, T. Hirono, and W. P. Huang, J. Lightwave Technol. **16**, 929 (1998).
- [4] F. Morichetti, A. Melloni, and M. Martinelli, J. Lightwave Technol. **24**, 573 (2006).
- [5] U. Wiedmann, P. Gallion, and G.-H. Duan, J. Lightwave Technol. **16**, 1343 (1998).
- [6] B. E. Little and S. T. Chu, IEEE Photonics Technol. Lett. **12**, 401 (2000).
- [7] S. S. A. Obayya, N. Somasiri, B. M. A. Rahman, and K. T. V. Grattan, Opt. Quantum Electron. **35**, 297 (2003).
- [8] A. Melloni, F. Morichetti, and M. Martinelli, Opt. Lett. **29**, 2785 (2004).
- [9] A. Melloni, R. Costa, P. Monguzzi, and M. Martinelli, Opt. Lett. **28**, 1567 (2003).
- [10] Wang Yun-ping and Zhang Dian-lin, Phys. Rev. A **52**, 2597 (1995).
- [11] H. Gersen, T. J. Karle, R. J. P. Engelen, W. Bogaerts, J. P. Korterik, N. F. van Hulst, T. F. Krauss, and L. Kuipers, Phys. Rev. Lett. **94**, 123901 (2005).